Web Crippling Design of Cold-formed Ferritic Stainless Steel Unlipped Channels with Web Holes and with Fastened Flanges Under End-two-flange loading Condition – Part I: Experimental Tests and Numerical Validation

Amir M. Yousefi, James B.P. Lim, and G. Charles Clifton

Department of Civil and Environmental Engineering, The University of Auckland, New Zealand

Abstract

Web holes are commonly used in beams of buildings to facilitate services. In this paper, a combination of tests and non-linear finite element analyses is used to investigate the effect of such web holes on the web crippling strength of cold-formed ferritic stainless steel unlipped channels under the end-two-flange (ETF) loading condition; the case of flanges fastened to the load and reaction plates is considered. The results of 27 web crippling tests are presented, with 9 tests conducted on unlipped channels without web holes and 18 tests conducted on unlipped channels with web holes. In the case of tests with web holes, the holes are located either centred or offset to the load and reaction plates. A quasi-static finite element model is then presented. Good agreement between the tests and finite element analyses is obtained in terms of failure load, failure modes and post-buckling behaviour.

Keywords

Cold-formed ferritic stainless steel; Finite element analysis; Unlipped channels; Web crippling; Web holes.

1   Introduction

Cold-formed ferritic stainless steels sections are becoming an increasingly attractive choice in buildings due to their combination of price, mechanical properties, and corrosion-resistance [1]. The material cost of stainless steel is largely dependent on the nickel content. Compared to austenitic and duplex grades, ferritic grades have no or very low nickel content, and thus have a lower material price [2]. When used as beams, to provide ease of access for services, the use of web holes are also becoming popular in industry [3] (see Fig. 1). Such web holes, however, result in the sections being more susceptible to web crippling, especially under concentrated loads in the vicinity of the holes and also influenced by the position of the holes.

Using the results of finite element static analyses, the Authors have recently proposed unified strength reduction factor equations for the web crippling strength of cold-formed stainless steel lipped channels with holes under the one and two flange loading condition covering three different stainless steel grades: duplex grade EN 1.4462; austenitic grade EN 1.4404 and ferritic grade EN 1.4003 [4-8]. Unlipped channels, however, were not considered, and no experimental tests were conducted. This paper both addresses these issues.

For stainless steel lipped channels, Krovink and van den Berg [11] and Krovink et al. [12] have considered lipped cold-formed stainless steel channels subject to one-flange loading. Zhou and Young [13-16] considered the web crippling strength of cold-formed stainless steel tubular sections, again without holes. Research by Lawson et al. [2], while concerned with web holes, focussed on the shear and bending capacity of the stainless steel lipped channels and not on the web crippling strength under concentrated loads. The Authors have also recently conducted experimental and numerical studies on cold-formed stainless steel unlipped channels subject to two-flange loading [17-19].

In terms of cold-formed carbon steel, Uzzaman et al. [20-23] have considered the web crippling strength of lipped channels under the two-flange loading condition. For web crippling without web holes, Poologanathan et al. [24] and Poologanathan and Mahendran [25] considered the web crippling strength of hollow flange channel beams, without holes in web. Lavan et al. [26] and Gunalan and Mahendran [27] have considered a Direct Strength Method approach in regard to the web crippling strength of lipped channels, again all without web holes.

In this study, a test programme was conducted on cold-formed ferritic stainless steel unlipped channels with web holes. The case of flanges fastened to the load and reaction plates are considered with the sections subject to end-two-flange (ETF) loading condition. The finite element modelling presented in this paper uses the general purpose finite element analysis program ABAQUS [28] for the numerical investigation. Web crippling design equations are presented in the companion paper [29].

Fig. 1   **Photograph of cold-formed stainless steel channel-sections with web holes after Lawson et al.** [2]

2   Experimental Investigation

2.1   Test sections

The ferritic stainless steel sheets (grade G430) were cut and press-braked to form unlipped channels for experimental study. In total, 27 unlipped channels having either web holes or without web holes were considered. In both cases, unlipped channels had three different depth sizes from 175mm to 250 mm with web slenderness ratio (h/t) between 148.92 and 232.63. The channels length (L) were chosen from the North American Specification (NAS) [30] where length equals 1.5 times height of the sections, plus length of the load or reaction plates. For channels with web holes, diameter (a) was between 68mm to 100mm. The cross-section dimensions measured in the lab as well as notations for determining the parameters are shown in Table 1 and Fig. 2 respectively. As can be seen in Fig. 3, the web holes were either in one end of the unlipped channels in between the load and reaction plates (centred holes) or in mid-length of the sections (offset holes). The unlipped sections are under exterior/external two flange load case where concentrated transverse load applies at the end of the unlipped channels.

**Table 1   The measured specimen details and experimental ultimate loads**

Specimen	Web d (mm)	Flange b_f (mm)	Thickness t (mm)	Fillet ratio r/t (mm)	Hole a (mm)	Length L (mm)	Experimental load per web P_{EXP} (kN)
175x60-t1.2-B50-A0	178.35	60.14	1.10	1.09	0.00	314.83	2.33
175x60-t1.2-B50-MA0.4	178.57	60.13	1.12	1.07	68.94	314.83	1.74
175x60-t1.2-B50-OA0.4	178.54	60.13	1.16	1.03	68.91	314.67	2.34
175x60-t1.2-B75-A0	178.56	60.06	1.15	1.04	0.00	339.50	2.96
175x60-t1.2-B75-MA0.4	178.38	60.07	1.08	1.11	68.72	339.67	1.91
175x60-t1.2-B75-OA0.4	178.56	60.07	1.12	1.07	68.74	339.67	2.59
175x60-t1.2-B100-A0	178.12	60.25	1.09	1.10	0.00	364.50	3.02
175x60-t1.2-B100-MA0.4	178.64	60.04	1.07	1.12	68.88	365.00	2.17
175x60-t1.2-B100-OA0.4	178.51	60.15	1.06	1.13	68.96	364.17	2.64
200x75-t1.2-B50-A0	203.55	74.97	1.16	1.03	0.00	349.33	2.41
200x75-t1.2-B50-MA0.4	203.65	75.01	1.10	1.09	78.93	349.17	1.50
200x75-t1.2-B50-OA0.4	203.62	75.04	1.15	1.04	78.94	349.33	2.19
200x75-t1.2-B75-A0	203.51	75.08	1.10	1.09	0.00	374.50	2.45
200x75-t1.2-B75-MA0.4	203.59	75.01	1.11	1.08	78.91	374.33	1.76
200x75-t1.2-B75-OA0.4	203.59	75.05	1.10	1.09	78.99	374.33	2.22
200x75-t1.2-B100-A0	203.56	75.04	1.09	1.10	0.00	379.50	2.65
200x75-t1.2-B100-MA0.4	203.57	75.01	1.06	1.13	78.81	400.00	1.82
200x75-t1.2-B100-OA0.4	203.62	74.97	1.05	1.14	78.82	399.00	2.24
250x100-t1.2-B50-A0	253.86	100.03	1.17	1.03	0.00	424.83	2.09
250x100-t1.2-B50-MA0.4	253.88	99.99	1.39	0.86	98.81	424.67	1.33
250x100-t1.2-B50-OA0.4	253.86	100.05	1.17	1.03	98.68	424.33	1.91
250x100-t1.2-B75-A0	253.57	99.96	1.16	1.03	0.00	450.00	2.28
250x100-t1.2-B75-MA0.4	253.50	99.92	1.10	1.09	98.78	450.00	1.39
250x100-t1.2-B75-OA0.4	253.48	100.02	1.13	1.06	98.83	449.67	1.96
250x100-t1.2-B100-A0	253.47	100.00	1.13	1.06	0.00	474.50	2.34
250x100-t1.2-B100-MA0.4	253.44	99.98	1.08	1.11	98.87	474.50	1.58
250x100-t1.2-B100-OA0.4	253.62	99.99	1.09	1.10	98.74	474.67	2.03

2.2   Specimens coding

In Tables1, the sections have been coded so that the nominal section dimension, the length of the load or reaction plates and web holes ratio (A) can be determined from the coding system. As an example, the label "175×60-t1.2-MA0.4-B100" can be explained as follows. The first and second annotations are the nominal sections depth and width in millimetres. Web holes ratio (A) are defined as measured depth of the web holes (a) over the measured depth of the plain part of the web (h) and can be one of 0.2, 0.4, 0.6 and 0.8; for example "A0.4" indicates a/h = 0.4. Unlipped sections without web holes are indicated by "A0". Also, the letter "M" indicates web holes are located in between the load and reaction plates and the letter "O" indicates that the web holes are in mid-length of the sections. The annotation "B100" indicates the load or reaction plate length in millimetres (i.e. 100 mm). The same definitions were used in the numerical investigation. The same definitions were used in the numerical investigation.
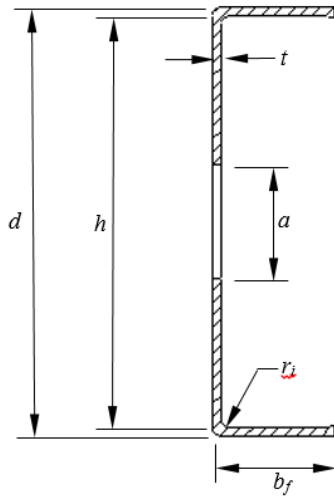
Fig. 2   Definition of symbols

(a) Offset web hole

(b) Centred web hole
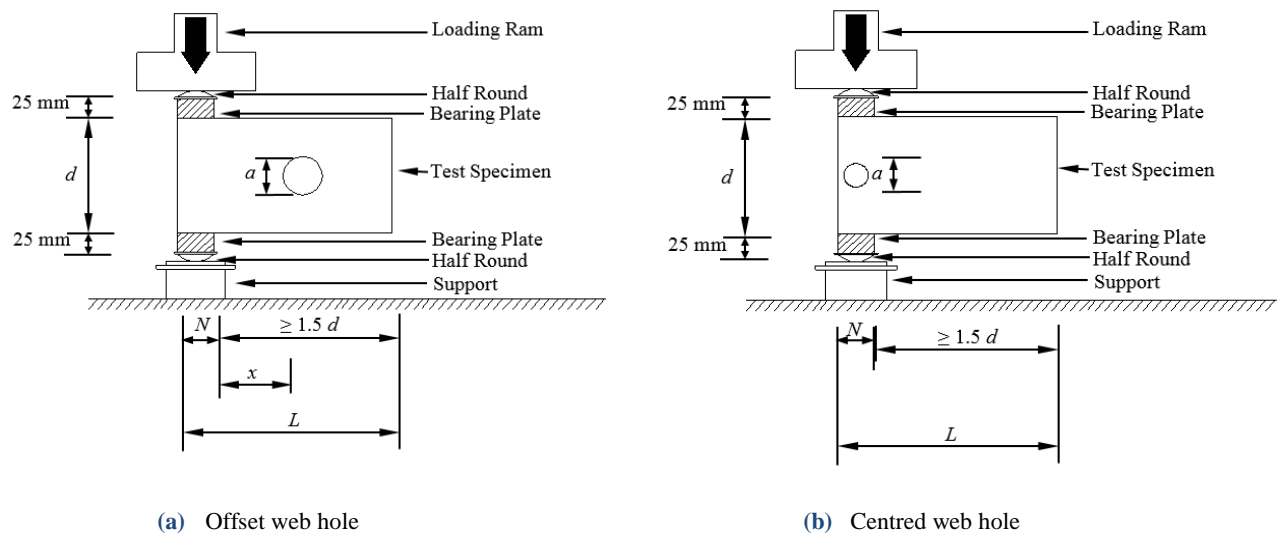
Fig. 3   Schematic front view of test set-up after Uzzaman et al. [20-23]

2.3   Material properties

Material testing was conducted on tensile coupons so to obtain the engineering stress-strain curve and mechanical properties of the test sections, as well as to develop numerical models of tested sections. The tensile coupons were prepared and tested in the Instron tensile testing machine according to ISO 6892-1:2009 [31]. Ten coupons were taken from both the longitudinal and transverse directions of the grade G430 ferritic stainless steel sheets from which the unlipped sections were fabricated. The average mechanical properties obtained from the ten coupon tests (five tests for each direction) are presented in Table 2. Comparative hot-rolled mechanical properties can be found in Yousefi et al. [32] and Rezvani et al. [33].

Table 2   The measured specimen details and experimental ultimate loads

| Section	Nominal Thickness (mm)	Base metal thickness (mm)	Gauge width (mm)	Gauge length (mm)	Yield stress $\sigma_{0.2}$ (MPa)	Tensile stress σ_u (MPa)
Longitudinal	1.2	1.18	20	141	276	452
Transverse	1.2	1.17	20	141	291	472
Average	---	---	---	---	284	462

2.4   Test set-up and procedure

The sections were tested under the ETF load case according to guidelines from NAS [30], as depicted in Fig. 3. Two identical steel plates of the same width and length applying concentrated forces were positioned at the bottom and top

flanges at the one end of each unlipped channel. Two half rounds, one at top and one at bottom, simulating pin supports were used in the line of action of transverse forces. An Instron machine with 100 kN capacity was used to employ a displacement load control to the test sections with a load ratio of 0.05 mm/min until failure. The transverse load was applied on the top plate and acted as the load plate. The reaction force was at the bottom plate. The load and reaction plates with 25mm thickness were made of high strength steel with 550 MPa yield stress. Three various lengths of load and reaction plates (100, 75 and 50 mm) were used in the laboratory study. Figs. 4-6 present the web crippling test-setup under ETF loading condition.

(a) Experimental   (b) FEA
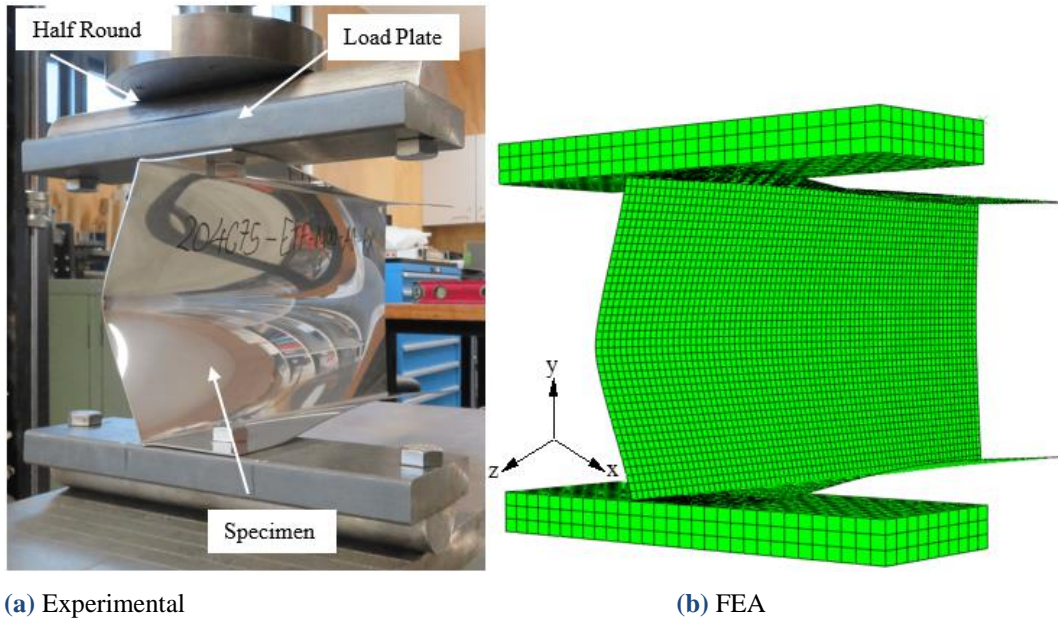
Fig. 4   Comparison of experiment and finite element analysis for without web hole

(a) Experimental   (b) FEA
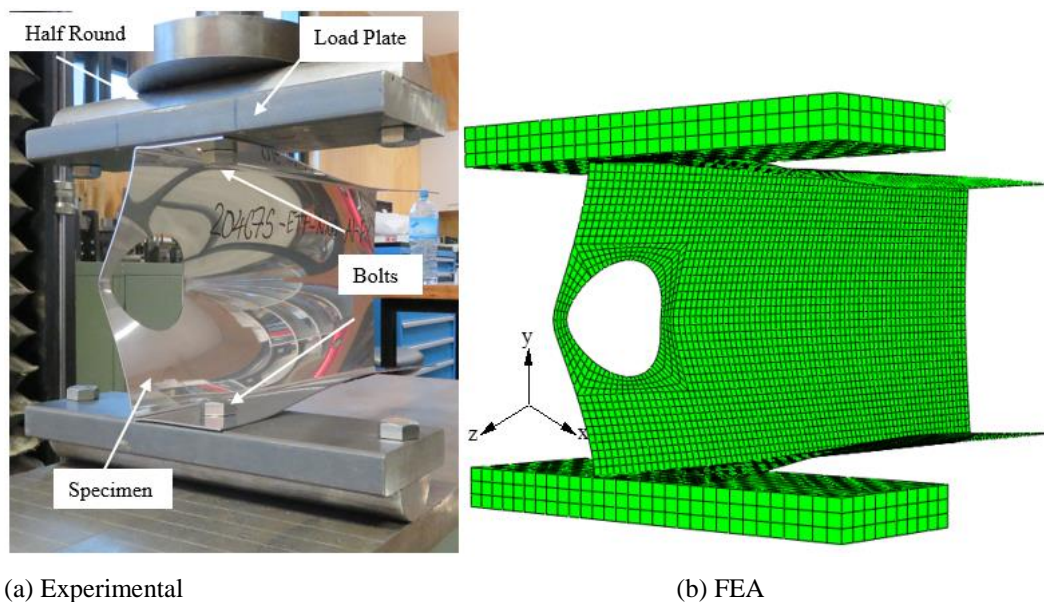
Fig. 5   Comparison of experiment and finite element analysis for centred web hole

(a) Experimental   (b) FEA
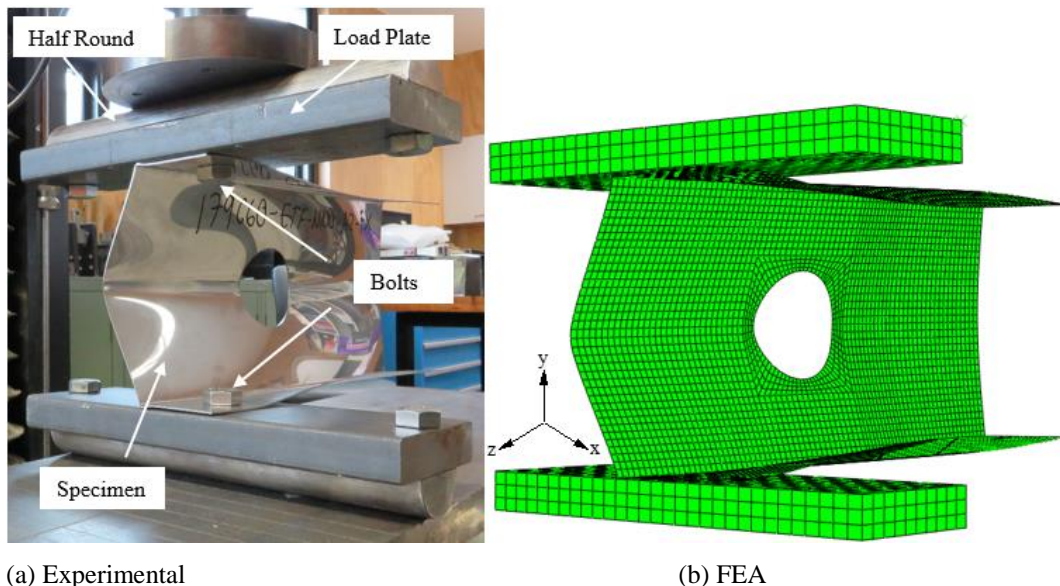
Fig. 6   Comparison of experiment and finite element analysis for offset web hole

2.5   Test results

In total, 27 unlipped channels were tested under the ETF loading condition where concentrated transverse load applies at the end of the sections. Table 1 presents the web crippling test ultimate loads per single web, defined as PLAB. Fig. 7 illustrates the typical web crippling failure mode of the sections, with web holes located either in between the load and reaction plates (centred hole) or in mid-length of the sections (offset hole). Also, typical load-displacement responses attained from the section 200×65-t1.2-N100, for both with and without web holes, can be seen in Fig. 8.

3   Numerical Investigation

In this paper, finite element (FE) models are also developed using the general application software ABAQUS [28] for the numerical investigation and the results presented in the parametric study. In previous studies [4-8], static general models were used. Hence, quasi-static models were used in this study as it was found that the elastic stiffness branch and post-buckling behaviour were better matched with the laboratory results; the ultimate loads, however, are generally unaffected.

(a) Without web hole
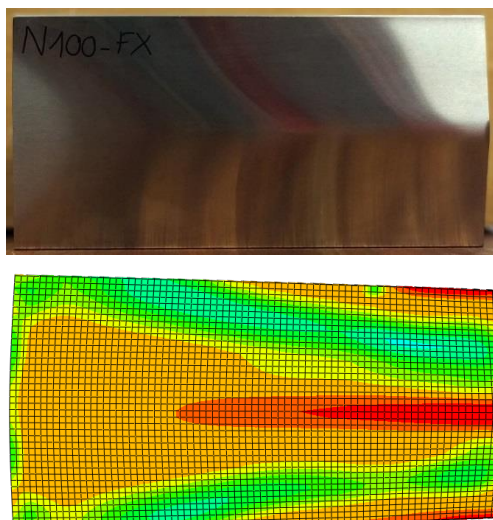
(b) Offset web hole   **(c)** Centred web hole
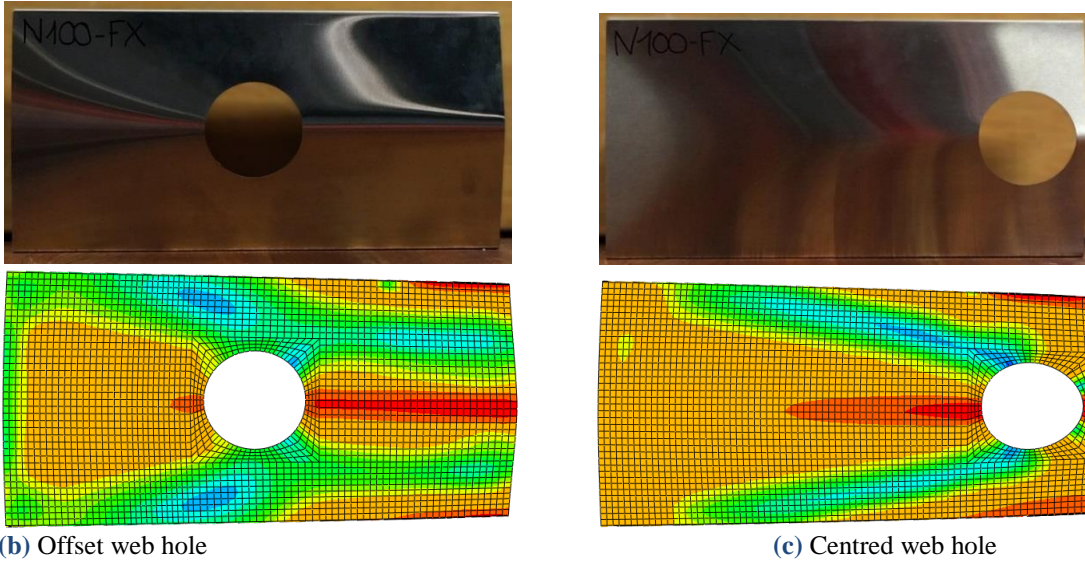
Fig. 7   **Typical failure modes of the specimens**
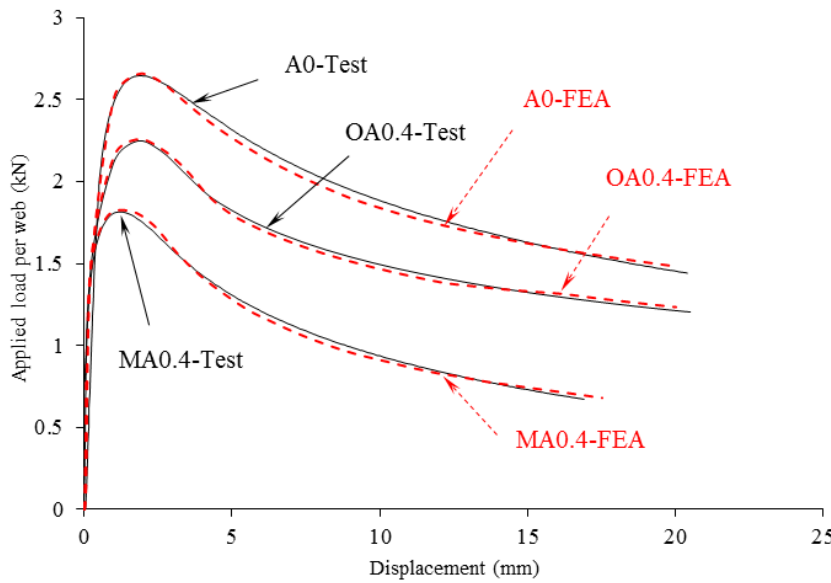
Fig. 8   **Comparison of web deformation curves for specimen 200×65-t1.2-B100**

3.1   Element type and material properties

The quadrilateral finite-membrain-strain S4R shell element was used for modelling the unlipped channels with and without holes in web. This general purpose three-dimensional element with 4-node doubly curved thin element is an appropriate element for most applications; especially for complex buckling behaviour, as it provides accurate and robust solutions. The general purpose hexahedral C3D8R solid element, appropriate for three-dimensional modelling, was used for modelling the load and reaction plates. The unlipped channels were modelled considering the centreline dimensions of the tested channels in the lab. The mean mechanical properties conducted from the tensile tests were also used for engineering stress-strain curve. As per ABAQUS manual [28], the engineering material curve is converted into true material curve in the FE modelling by using the following equations:

$$\sigma_{true} = \sigma \left(1 + \varepsilon\right) \tag{1}$$

$$\varepsilon_{true(pl)} = \ln(1 + \varepsilon) - \frac{\sigma_{true}}{E} \tag{2}$$

3.2   Geometry and mesh

Figs. 4-6 show the full scale of laboratory test set-up modelled in the numerical study. The typical finite element mesh of the unlipped channels as well as load and reaction plates are shown in Figs. 4-6. Finite element mesh sizes of 8 × 8 mm were used for the load and reaction plates and 5 × 5 mm for the unlipped channels. At least five elements were

used for meshing the corner region of the channels due to transferring transverse loads from flanges to web. For modelling unlipped channels with web holes, structured mesh with at least five elements was applied around the holes.

Table 3   Web crippling strength comparison from test results and predicted from finite element analysis

Specimen	Web slenderness ratio (h/t)	Hole diameter ratio (a/h)	Exp. load per web P_{EXP}(kN)	Web crippling strength per web predicted from FEA P_{FEA}(kN)	Comparison P_{EXP}/P_{FEA}
175x60-t1.2-B50-A0	150.38	0.00	2.33	2.30	1.01
175x60-t1.2-B50-MA0.4	154.54	0.39	1.74	1.76	0.99
175x60-t1.2-B50-OA0.4	151.84	0.39	2.34	2.37	0.99
175x60-t1.2-B75-A0	154.53	0.00	2.96	2.97	1.00
175x60-t1.2-B75-MA0.4	149.14	0.39	1.91	1.88	1.03
175x60-t1.2-B75-OA0.4	153.18	0.39	2.59	2.62	0.99
175x60-t1.2-B100-A0	155.50	0.00	3.02	3.01	1.00
175x60-t1.2-B100-MA0.4	153.25	0.39	2.17	2.17	1.00
175x60-t1.2-B100-OA0.4	154.48	0.39	2.64	2.63	1.00
200x75-t1.2-B50-A0	171.92	0.00	2.41	2.41	1.00
200x75-t1.2-B50-MA0.4	169.12	0.39	1.50	1.49	1.01
200x75-t1.2-B50-OA0.4	173.47	0.39	2.19	2.18	1.00
200x75-t1.2-B75-A0	171.89	0.00	2.45	2.43	1.01
200x75-t1.2-B75-MA0.4	201.19	0.39	1.76	1.77	0.99
200x75-t1.2-B75-OA0.4	176.48	0.39	2.22	2.24	0.99
200x75-t1.2-B100-A0	179.61	0.00	2.65	2.65	1.00
200x75-t1.2-B100-MA0.4	178.03	0.39	1.82	1.83	0.99
200x75-t1.2-B100-OA0.4	181.28	0.39	2.24	2.25	1.00
250x100-t1.2-B50-A0	211.31	0.00	2.09	2.10	1.00
250x100-t1.2-B50-MA0.4	204.46	0.39	1.33	1.33	1.00
250x100-t1.2-B50-OA0.4	213.10	0.39	1.91	1.92	0.99
250x100-t1.2-B75-A0	209.31	0.00	2.28	2.31	0.99
250x100-t1.2-B75-MA0.4	209.25	0.39	1.39	1.39	1.00
250x100-t1.2-B75-OA0.4	218.33	0.39	1.96	1.98	0.99
250x100-t1.2-B100-A0	212.77	0.00	2.34	2.33	1.01
250x100-t1.2-B100-MA0.4	232.44	0.39	1.58	1.57	1.01
250x100-t1.2-B100-OA0.4	220.37	0.39	2.03	2.01	1.01
Mean					1.00
COV					0.01

3.3   Boundary conditions and loading procedure

An analytical solid plate was used to simulate the load plate with a reference point constraining the top surface of the load plate. The load plate was prevented from all translational and rotational movements, excluding vertical y translation. The vertical displacement in y direction was applied to the load plate through the reference transferring displacement load through the load plate to the unlipped channel. The unlipped channels with web holes, load and reaction plates, and the interfaces between the unlipped channels and the load and reaction plates were modelled.

"Surface to surface" contact was used for contact modelling between the load and reaction plates and channel flanges in ABAQUS. The flanges of the unlipped channels were the slave surface, while the load and reaction plates were the master surfaces. Penetration was not allowed between the two contact surfaces. Isotropic friction was adopted between the surfaces using penalty formulation and a friction coefficient equivalent to µ=0.4.

3.4　Finite element (FE) verification

The laboratory and the finite element (FE) results were compared to determine the suitability of the models. The obtained results from web crippling test ultimate loads per single web (PEXP) and the web bearing FEA ultimate loads per single web (PFEA) are presented in Table 3. It is clear from Table 3 that the mean ratio of the laboratory results over FE results stances 1.00 having the coefficient of variation of COV=0.01. Overall, 3% was the maximum difference for the section 175x60-t1.2-B75-MA0.4 obtained from the FE and laboratory results. Fig. 8 presents the comparison of the load-displacement responses for section 200×65-t1.2-B100 for unlipped channels without and with holes in web. A good agreement has been attained for both sections without and with holes in web. Finally, as depicted in Fig. 7, the failure modes from the tested sections subjected to the ETF loading condition have been compared and validated against the FE model. The failure modes from the finite element results were observed to be similar to the experimental failure modes of the sections.

4　Conclusions

In this paper, a combination of tests and non-linear finite element analyses was used to investigate the effect of web holes on the web crippling strength of cold-formed ferritic stainless steel unlipped channels under the end-two-flange (ETF) loading condition; the case of flanges fastened to the load and reaction plates is considered. The results of 27 web crippling tests were presented, with 9 tests conducted on unlipped channels without web holes and 18 tests conducted on unlipped channels with web holes. In the case of tests with web holes, the holes are located either centred or offset to the load and reaction plates. The unlipped channels had the measured 0.2% proof stress (yield stress) of 276 MPa and 291 MPa in two sheet directions. The web slenderness values ranged from 154.25 to 251.75. The ratio of the diameter of the holes to the depth of the plain part of the webs (*a/h*) was kept constant 0.4 in order to investigate the influence of the web holes on the web crippling behaviour. Flanges of the unlipped channels were fastened to the load and reaction plates.

Quasi-static finite element models were then used and verified against the experimental results in terms of web crippling failure loads, the failure modes and post-buckling behaviour. The finite element models provided a good prediction for web crippling strength of cold-formed ferritic stainless steel unlipped channels with and without web holes. The verified finite element models can be used to carry out an extended study for developing reliable design recommendations for cold-formed stainless steel unlipped channels.

References

[1]　K. A. Cashell, N. R. Baddoo, Ferritic stainless steels in structural applications, Thin-Walled Structures, 83 (2014) 169-181.

[2]　N.R. Baddoo, Stainless steel in construction: A review of research, applications, challenges and opportunities, Journal of Constructional Steel Research, 64 (2008), 1199-1206.

[3]　R. M. Lawson, A. Basta, A. Uzzaman, Design of stainless steel sections with circular openings in shear, Journal of Constructional Steel Research, 112 (2015) 228-241.

[4]　A.M. Yousefi, J.B.P. Lim, A. Uzzaman, Y. Lian, G.C. Clifton, B. Young, Web crippling strength of cold-formed stainless steel lipped channel-sections with web openings subjected to Interior-One-Flange loading condition, Steel and Composite Structures, 21 (2016) 629-659.

[5]　A.M. Yousefi, J.B.P. Lim, A. Uzzaman, Y. Lian, G.C. Clifton, B. Young, Web Crippling Strength of Cold-Formed Duplex Stainless Steel Lipped Channel-Sections with Web Openings Subjected to Interior-One-Flange Loading Condition, Proceeding of The Wei-Wen Yu International Specialty Conference on Cold-Formed Steel Structures, Missouri University of Science and Technology-Rolla, Missouri, (2016) 313-324.

[6]　A.M. Yousefi, J.B.P. Lim, A. Uzzaman, Y. Lian, G.C. Clifton, B. Young, Design of cold-formed stainless steel lipped channel-sections with web openings subjected to web crippling under End-One-Flange loading condition, Advances in Structural Engineering, 20 (2017) 1024-1045.

[7]　A.M. Yousefi, A. Uzzaman, J.B.P. Lim, G.C. Clifton, B. Young, Numerical investigation of web crippling strength in cold-formed stainless steel lipped channels with web openings subjected to interior-two-flange loading condition, Steel and Composite Structures, 23 (2017) 363-383.

[8]　A.M. Yousefi, A. Uzzaman, J.B.P. Lim, G.C. Clifton, B. Young, Web crippling strength of cold-formed stainless steel lipped channels with web perforations under end-two-flange loading, Advances in Structural Engineering, DOI: 10.1177/1369433217695622.

[11] S.A. Korvink, G.J. van den Berg, Web crippling of stainless steel cold-formed beams. Proceeding of The 12th International Specialty Conference on Cold-Formed Steel Structures, University of Missouri-Rolla, St. Louis, (1994) 551-569.

[12] S.A. Korvink, G.J. van den Berg, P. van der Merwe, Web crippling of stainless steel cold-formed beams, Journal of Constructional Steel Research, 34 (1995) 225-248.

[13] F. Zhou, B. Young, Yield line mechanism analysis on web crippling of cold-formed stainless steel tubular sections under two-flange loading, Engineering Structures, 28 (2006) 880-892.

[14] F. Zhou, B. Young, Cold-formed high-strength stainless steel tubular sections subjected to web crippling, Journal of structural engineering, 133 (2007) 368-377.

[15] F. Zhou, B. Young, Web crippling behaviour of cold-formed duplex stainless steel tubular sections at elevated temperatures, Engineering Structures, 57 (2013) 51-62.

[16] F. Zhou, B. Young, Web crippling of aluminium tubes with perforated webs, Engineering Structures, 32 (2010) 1397-410.

[17] A.M. Yousefi, J.B.P. Lim, G.C. Clifton, Cold-formed ferritic stainless steel unlipped channels with web openings subjected to web crippling under interior-two-flange loading condition - part I: tests and finite element model validation. Thin-Walled Structures, 116 (2017) 333-341.

[18] A.M. Yousefi, J.B.P. Lim, G.C. Clifton, Cold-formed ferritic stainless steel unlipped channels with web openings subjected to web crippling under interior-two-flange loading condition - part II: Parametric study and design equations. Thin-Walled Structures, 116 (2017) 342-356.

[19] A.M. Yousefi, J.B.P. Lim, G.C. Clifton, Web bearing capacity of unlipped cold-formed ferritic stainless steel channels with perforated web subject to end-two-flange (ETF). Engineering Structures 2017, [under review].

[20] A. Uzzaman, J.B.P. Lim, D. Nash, J. Rhodes, B. Young, Web crippling behaviour of cold-formed steel channel sections with offset web holes subjected to interior-two-flange loading, Thin-Walled Structures, 50 (2012) 76-86

[21] A. Uzzaman, J.B.P. Lim, D. Nash, J. Rhodes, B. Young, Effect of offset web holes on web crippling strength of cold-formed steel channel sections under end-two-flange loading condition, Thin-Walled Structures, 65 (2013) 34-48.

[22] A. Uzzaman, J.B.P. Lim, D. Nash, J. Rhodes, B. Young, Cold-formed steel sections with web openings subjected to web crippling under two-flange loading conditions-part I: tests and finite element analysis, Thin-Walled Structures, 56 (2012) 38- 48.

[23] A. Uzzaman, J.B.P. Lim, D. Nash, J. Rhodes, B. Young, Cold-formed steel sections with web openings subjected to web crippling under two-flange loading conditions-part II: Parametric study and proposed design equations, Thin-Walled Structures, 56 (2012) 79- 87.

[24] K. Poologanathan, M. Mahendran, E. Steau, Experimental study of web crippling behaviour of hollow flange channel beams under two flange load cases, Thin-Walled Structures, 85 (2014) 207-219.

[25] K. Poologanathan, M. Mahendran, Experimental study of web crippling behaviour of hollow flange channel beams under two flange load cases, Advances in Structural Engineering, 19 (2016) 966-981.

[26] S. Lavan, M. Mahendran, K. Poologanathan, Experimental studies of lipped channel beams subject to web crippling under two-flange load cases, Journal of Structural Engineering, 142 (2016) 04016058.

[27] S. Gunalan, M. Mahendran, Web crippling tests of cold-formed steel channels under two flange load cases, Journal of Constructional Steel Research, 110 (2015) 1-15.

[28] ABAQUS Analysis User's Manual-Version 6.13-1. ABAQUS Inc., USA, 2014.

[29] A.M. Yousefi, J.B.P. Lim, G.C. Clifton, Web crippling design of cold-formed ferritic stainless steel unlipped channels with web holes and with fastened flanges under end-two-flange loading condition-part I: Experimental tests and numerical validation. *Stainless Steel in Structures – Fifth International Experts Seminar,* London, UK, (2017), [submitted].

[30] NAS, North American Specification for the Design of Cold-Formed Steel Structural Members, American Iron and Steel Institute, AISI S100-2016, AISI Standard, 2016.

[31] ISO E. 6892-1, Metallic Materials–Tensile Testing—Part 1: Method of Test at Room Temperature ISO E. 6892-1, International Standard, Geneva (2009).

[32] A.M. Yousefi, M. Hosseini, N. Fanaie, Vulnerability Assessment of Progressive Collapse of Steel Moment Resistant Frames, Trends in Applied Sciences Research, 9 (2014) 450-460.

[33] F.H. Rezvani, A.M. Yousefi, H.R. Ronagh, Effect of span length on progressive collapse behaviour of steel moment resisting frames, Structures, 3 (2015) 81-89.